View Article Online
View Journal

Chemical
Science

This article can be cited before page numbers have been issued, to do this please use: C. Li, L. Yang, Y. Li, J. Liu and Y. Chen, *Chem. Sci.*, 2026, DOI: 10.1039/D6SC03246J.

ROYAL SOCIETY
OF CHEMISTRY

rsc.li/chemical-science

View Article Online
DOI: 10.1039/D6SC03246J

ARTICLE

Dichroic Dyes Mediated Mirrored Full-Color and White Circularly Polarized Luminescence in Natural Cholesteric Liquid Crystals Systems

Received 00th January 20xx,
Accepted 00th January 20xx

DOI: 10.1039/x0xx00000x

Chenlan Li,[a] Linda Yang,[a] Yang Li,[b] Jianquan Liu*[a] and Yihan Chen*[a]

Natural chiral dopants have been widely employed in liquid crystal displays, biomedicine, and chiral optical materials owing to their easy availability of chirality and excellent biocompatibility. However, most natural chiral compounds exist exclusively as single enantiomer, which severely restricts their application scope in circularly polarized luminescence (CPL). Herein, we design and synthesize a class of full-color dichroic dyes capable of modulating the handedness of CPL signals without relying on chiral dopants. In natural chiral dopant-incorporated cholesteric liquid crystal (CLC) systems, these dyes with a unique excited-state intramolecular proton transfer (ESIPT) isomeric structure achieve mirror-symmetric full-color and white CPL. This work expands the application of natural chiral compounds in CPL materials and provides a novel, sustainable strategy for high-performance CPL devices and flexible optical displays.

Introduction

Circular polarization describes the spatial rotation of light waves as they propagate over time, enabling precise control over the emission spectral distribution and propagation behavior.[1-3] This unique characteristic endows circularly polarized luminescence (CPL) materials with immense application potential in frontier fields such as 3D displays, visible light communication systems, and high-security encryption technologies.[4-6] Thus, research on CPL-active materials has garnered significant attention in recent years, with intensive efforts focused on optimizing their key performance metrics. Currently, one of the primary challenges is achieving CPL materials with a high dissymmetric factor ($|g_{\mathrm{lum}}|$), a critical parameter that directly determines the efficiency of chiral light emission and practical applicability.[7, 8]

Emissive cholesteric liquid crystals (CLC) have emerged as a versatile and effective platform for realizing high $|g_{\mathrm{lum}}|$ values, leveraging the chiral supramolecular co-assembly of their components.[9-11] Notably, CLC can be readily fabricated via two common strategies: either doping chiral inducers (chiral dopants) into nematic liquid crystals (NLC)[12, 13] or via the self-assembly of chiral liquid crystal molecules themselves.[14, 15] Among these approaches, the utilization of natural chiral compounds as dopants has garnered particular interest due to their intrinsic biocompatibility, structural diversity, and cost-efficiency.[16-18] When CLC form an ordered periodic helical superstructure, they can act as a chiral microenvironment. Upon incorporation of achiral dichroic dyes into this matrix, intermolecular chirality transfers and induction effects take place between the CLC host and guest dyes, leading to significant amplification of the CPL signal.[19, 20]

However, a critical limitation of natural chiral dopants lies in their inherent single-handedness. Most natural chiral molecules (e.g., amino acids, sugars, and cholesterol derivatives) exist predominantly in only one enantiomeric form, with the opposite enantiomer often being costly to synthesize or even commercially unavailable.[21, 22] This constraint greatly restricts the flexible design, performance optimization, and practical deployment of CPL materials, since the handedness of CPL in CLC systems is usually governed by the helical direction of the CLC matrix, which is fixed by the dopant chirality. Therefore, it is crucial to develop strategies enabling independent control over CPL handedness without relying on the synthesis of opposite enantiomers of chiral dopants.

Recent studies indicate that dichroic dyes possess the unique capability to modulate the handedness of CPL emission, even when embedded in a CLC host with a fixed spiral direction.[23-25] Building on this insight, herein we designed a series of dichroic molecules with different emission wavelengths covering red, green, and blue regions, which possess ESIPT properties enabling the modulation of dichroism. By incorporating these dyes into CLC derived from a single natural chiral dopant (cholesterol derivative), we successfully achieved full-color and mirror-image CPL covering the visible range, as well as white circularly polarized luminescence (WCPL), as shown in Scheme 1. This strategy not only circumvents the limitation of the single-handedness of natural chiral dopants but also provides a simple, cost-effective route to full-color and white CPL materials, holding great promise for advancing their practical applications.

---

[a] School of Chemistry and Materials Science, Jiangsu Key Laboratory of Green Synthesis for Functional Materials, Jiangsu Normal University, Xuzhou, Jiangsu 221116, China. Email: liujq316@jsnu.edu.cn; 6020240050@jsnu.edu.cn.
[b] Wenzhou Key Laboratory of Biophysics, Wenzhou Institute, University of Chinese Academy of Sciences, Wenzhou 325000, P. R. China. Email: liyangchem@foxmail.com.

Supplementary Information available: See DOI: 10.1039/x0xx00000x

View Article Online
DOI: 10.1039/D6SC03246J

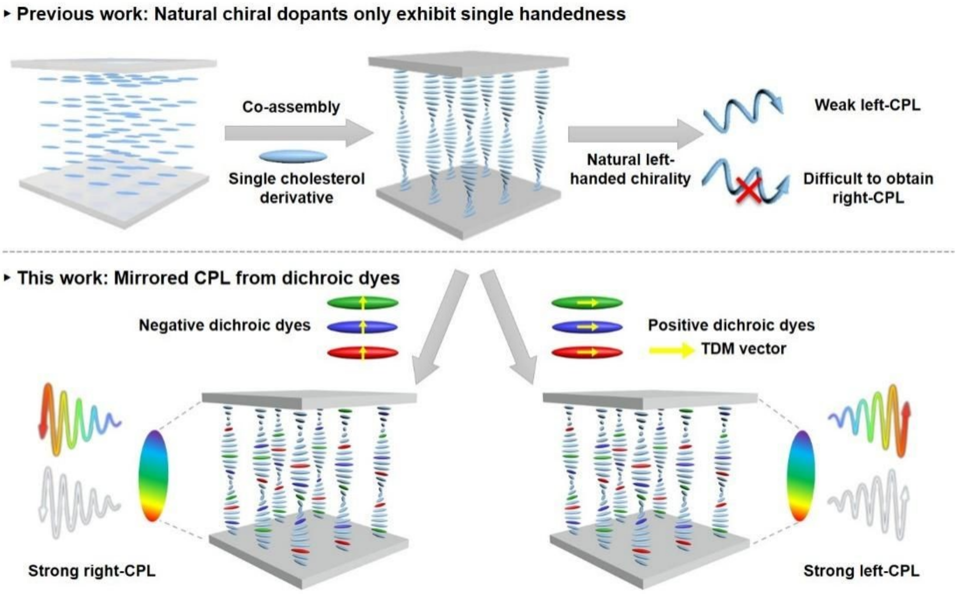

Scheme 1. Comparison of CPL achieved in co-assembled CLC: Conventional naturally chiral dopant-induced CLC with single handedness versus full-color dichroic dye-mediated CLC systems with mirror-symmetric CPL signals.

Results and discussion

Photophysical properties

A series of excited-state intramolecular proton transfer (ESIPT)-active dichroic dyes were synthesized by introducing distinct substituents Ar_n (Fig. 1a) onto the core skeleton of imidazole-phenanthrenequinone isomers, yielding compounds P1, P2, P3 and N1, N2, N3, respectively. The detailed synthesis procedures and characterization of these molecules are provided in the Supporting Information (Experimental Section, Fig. S12-24 and Table S1). The optical properties of these compounds were studied in tetrahydrofuran (THF) solution at a concentration of 10^{-5} mol/L. Emission spectroscopy measurements revealed that the ESIPT molecules P1, P2, and P3 exhibit characteristic emission peaks at 430 nm, 507 nm, and 563 nm, respectively (Fig. 1b). Similarly, the isomeric molecules N1, N2, and N3 display identical emission maxima at 430 nm, 507 nm, and 563 nm, respectively, which is attributed to their identical isomeric molecular skeletons. In the ground state, these dyes exist in the enol form. Upon excitation, intramolecular proton transfer occurs, producing the keto form in the excited state and resulting in a large apparent Stokes shift.[14, 26, 27] Notably, the absorption spectra of these ESIPT derivatives are all confined to the UV region (Fig. 1c). As a result, there is almost no spectral overlap between their absorption and emission bands and thus minimizing the self-absorption of the molecules.

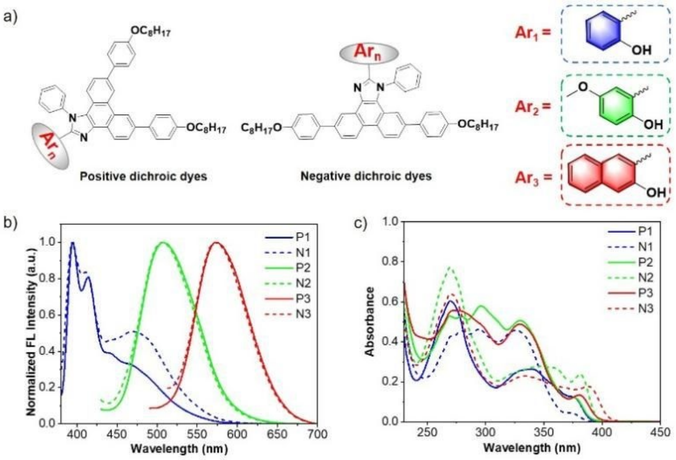

Fig. 1. a) The molecular structure of dichroic dyes isomers in CLC system; b) Emission spectra and c) UV-*vis* absorption of positive and negative dichroic dyes.

Dichroic properties

To verify the dichroism of the three dyes, the polarization fluorescence (FL) spectra of achiral dyes in liquid-crystal media were quantitatively measured and described by the S_F values.[28-30] The emissive NLC systems, NLC-P1~P3 and NLC-N1~N3, were prepared by doping 1 wt% of dichroic dyes P1~3 and N1~3 into the commercial NLC E7 respectively. After injecting the NLC into aligned liquid crystal cells, the FL spectra parallel ($F_{/\!/}$) and perpendicular ($F_{\perp}$) to the molecular orientation were measured, as shown in Fig. 2a, 2b and Fig. S1. The stronger $F_{/\!/}$ emission intensity confirmed the positive dichroic nature of P1~P3, with an S_F value of 0.08, 0.18 and 0.41

View Article Online
DOI: 10.1039/D6SC03246J

(Equation S1). The stronger $F_{\perp}$ emission intensity of N1~3 indicated their negative dichroic properties, with S_F values of -0.09, -0.27 and -0.40, respectively. Notably, the S_F values of P1~2 and N1~2 in E7 are lower than those of P3/N3. This difference can be ascribed to the more extended conjugated backbone of P3/N3, which strengthens intermolecular interactions with the E7 host and thereby gives rise to a higher orientational order. Accordingly, dichroic dyes with high S_F can be achieved via rational structural engineering of ESIPT-active dichroic molecules.

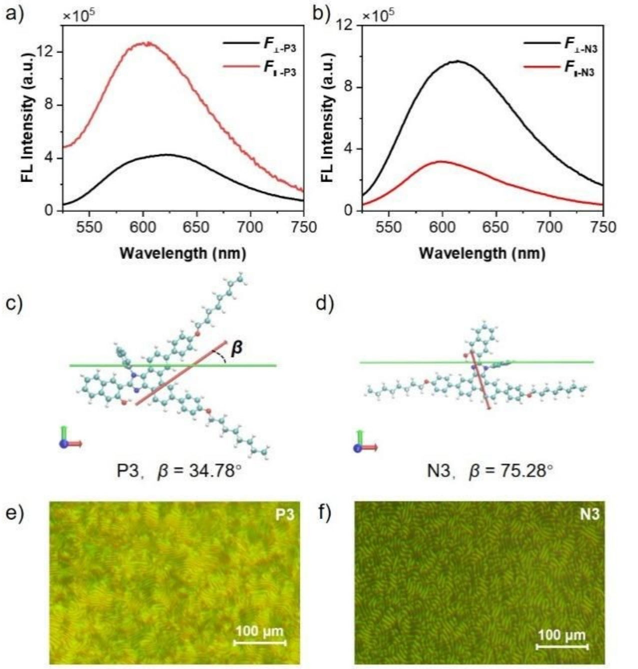

Fig. 2. a) Polarized FL spectra of the NLC-P3 and b) NLC-N3; c) DFT calculation of the molecules P3 and d) N3 (red arrow indicates the TDM vector and green rod indicates the MOI axis); e) POM images of *S*-CLC-P3 and f) *S*-CLC-N3.

To investigate the origin of the difference between these positive and negative dichroic behavior of the achiral dyes, we performed density functional theory (DFT) calculations using the B3LYP/6-31G method with the Gaussian 09 program.[31] The results, shown in Fig. 2c, 2d and Fig. S2, revealed that the transition dipole moment (TDM) vectors for the ESIPT dyes extend from the imidazole group to the carbonyl group. Fundamentally, a smaller angular deviation between the molecular orientation axis (MOI) and the TDM vector corresponds to a higher S_F value.[24] Based on this principle, the molecular design of N1~N3 was implemented by anchoring mesogenic units onto the imidazoline ring in a direction perpendicular to the TDM vector, thereby amplifying their negative dichroism. In contrast, the mesogenic groups of P1~P3 were conjugated to the imidazoline ring parallel to the TDM orientation, which endows these dyes with positive dichroic dichroism. Basically, the theoretical calculation results demonstrate that the molecular design and structural features of ESIPT molecules enable the effective regulation of their dichroic properties.

To construct natural chiral-derived CPL-active CLC materials, commercially available cholesteryl oleyl carbonate (C1, a representative cholesterol derivative) was utilized as the chiral dopant, and emissive CLC composites were fabricated by doping C1 together with achiral dichroic dyes into commercial NLC E7. Taking P2 as a reference, LC cell thickness and the doping concentrations of the chiral inducer and achiral dyes were optimized (Fig. S3 and S9). A characteristic fingerprint texture was observed in the POM images of the CLC (Fig. 2e, 2f and Fig. S4), indicating the formation of a highly ordered helical superstructure through the co-assembly process. The helical pitches were calculated to be 7.59, 8.28, 7.03, 7.71, 7.74 and 7.15 μm, respectively, which are evidently larger than the range of the visible light region (Fig. 3a, b and Fig. S6). Based on these measurements, we can rule out the possibility that the effect of selective reflection plays a role in the CPL emission.[9, 32-34] The handedness of the helix was confirmed by comparing the CLC to natural cholesteryl oleyl carbonate, which is known to exhibit a left-handed structure.[35-36] As shown in Fig. 3c, d and Fig. S7, all CLC-P1~P3 and CLC-N1~N3 exhibited a left-handed helix with a continuous pattern at the contact zones of the CLC and cholesteryl oleyl carbonate. These results reveal achiral dichroic dyes hardly change the CLC superstructure, demonstrating their dichroism modulate CPL polarization without disrupting the helical structure.

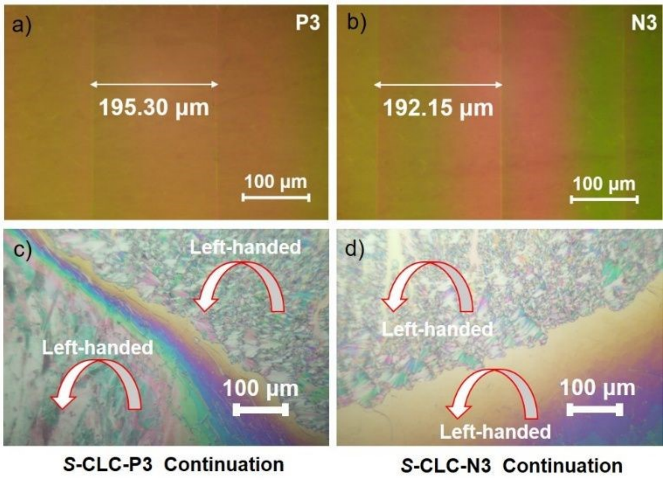

Fig. 3. POM images of a) *S*-CLC-P3, b) *S*-CLC-N3 in wedge liquid crystal cells; Miscibility test of c) *S*-CLC-P3 and d) *S*-CLC-N3 induced by cholesteryl oleyl carbonate.

Chiroptical properties

Emissive CLC were then prepared by doping 1.5 wt% of P1~P3 and N1~N3 into the E7 host containing 1.5 wt% of cholesteryl oleyl carbonate, respectively, then injected them into 15 μm thick quartz cells. The chiroptical properties of these CLC in the ground states were further investigated. The circular dichroism (CD) spectra of all these CLC revealed a strong mirror-image effect and significant Cotton effects from 280 to 400 nm (Fig. 4a). The band at 310 nm is attributed to the chiral co-assembly between the CLC host and achiral dyes, indicating that they share the same helical superstructure in the CLC host. The strong absorption at 380 nm corresponds to the absorption of the achiral dichroic dyes themselves. These pronounced CD signals are the result of efficient chiral transfer from the CLC host to the achiral dyes during the co-assembly process.[37] However, the CD signals of S-CLC-P1~P3 and *S*-CLC-N1~N3 exhibited opposite polarization in the range of 370 to 400 nm, which is likely due to the inverted TDM helix induced by the different dichroism nature of the ESIPT dyes.[38, 39]

To further elucidate the chiroptical performance of the co-assembled CLC systems, the intrinsic chiral excited-state characteristics of the CLC systems were evaluated via CPL spectroscopy. For CLC-P1~P3, strong positive CPL signals were observed, with g_{lum} values of −0.23 at 425 nm, −0.28 at 524 nm, and −0.29 at 605 nm (Fig. 4b), which were in good agreement with CLC emission spectra (Fig. S5). In contrast, CLC-N1~N3 displayed strong negative CPL signals, with g_{lum} values of 0.21 at 476 nm, 0.28 at 525 nm, and 0.30 at 608 nm, which was highly consistent with their CD spectral trends. Importantly, despite using the same chiral inducer, CLC-N1~N3 exhibited opposite CPL polarizations compared to CLC-P1~P3. This behavior can be attributed to the different the TDM vectors of achiral dichroic dyes. Notably, CPL intensities of the CLC correlated well with the S_F values of the corresponding dyes. *S*-CLC-P3/N3 exhibited the strongest CPL emission, owing to efficient chirality transfer from chiral dopant C1 to high-S_F of P3/N3 in the CLC medium. These results confirm that rational modulation of ESIPT sites tunes dichroic properties of achiral dichroic dyes in CLC, enabling effective CPL regulation without altering the superstructure of the CLC host. The occurrence of linear dichroism/linear birefringence effect was ruled out by observing no change in the CPL spectrum upon sample rotation and flipping (on the front and back sides of the flat cells, Figure S10).

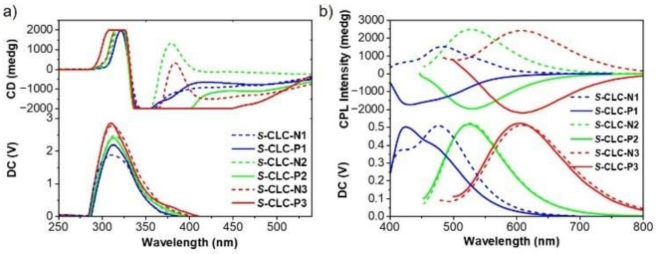

Fig. 4. a) CD and b) CPL spectra of *S*-CLC-N1-N3 and *S*-CLC-P1-P3.

WCPL properties

White circularly polarized luminescence (WCPL) integrates circular polarization and broadband white emission, attracting considerable attention due to its promising applications in information storage, biomedicine, and optoelectronic devices.[40-42] Conventional CLC-based WCPL relies on enantiomeric chiral dopant doping[43-45], making it challenging to obtain mirrored WCPL using a single natural chiral dopant and thus limiting the application of natural chiral molecules.

Herein, we achieve mirror-symmetric WCPL in CLC with a single natural chiral dopant (C1) by adjusting the ratio of full-color dichroic dyes. Specifically, white-light-emitting *S*-CLC-W1 with positive CPL signals was prepared by tuning the ratio of N1~N3 (1:0.1:2.1 wt%) in E7 liquid crystals (LC) doped with 1.5% C1. While *S*-CLC-W2 with negative CPL signals was obtained by adjusting the ratio of P1~P3 (1:0.23:2.3 wt%) in the same C1-doped E7 LC. Both ternary *S*-CLC-W1 and *S*-CLC-W2 retained obvious fingerprint textures (Fig. S8), confirming the formation of stable CLC phases. Under 365 nm excitation, both samples exhibited four emission peaks at 395, 422, 488, and 581 nm, originating from E7 and the N1~N3/P1~P3 dyes, respectively (Fig. 5a).The fluorescence quantum yields of CLC-W1 and CLC-W2 were 6.5% and 5.6%, with chromaticity coordinates (CIE) centered at (0.32, 0.34) and (0.31, 0.33), respectively (Fig. 5b). These results verify that the constructed CLC systems achieve stable white-light emission with well-defined chromaticity. Notably, *S*-CLC-W1 and *S*-CLC-W2 showed distinct mirror-image CPL signals in the 400-750 nm range (Fig. 5c), consistent with the fluorescence emission of the achiral dyes (Fig. 1b), and their $|g_{lum}|$ values ranged from 0.2 to 0.4 (Fig. 5d), which are considerably larger than those of previously reported white CPL-active materials.[46-49] Therefore, This type of standard mirror-image and white CPL with desirable $|g_{lum}|$ values can be generated through the highly ordered helical stacking of these full-color dichroic dyes, mediated by the co-assembly of CLCs with only one natural chiral dopant. Then we investigated the CPL variations of CLC-W1 and CLC-W2 under an external electric field for practical device applications. Upon applying 8 V voltage, the CPL signal dropped to nearly zero. This performance could be rapidly restored over 5 cycles with negligible attenuation. The change of CPL signals under external electric field originates from the transformation of the CLC superstructure: the planar chiral arrangement converts to a vertical nematic phase(Fig. S11 and S12).

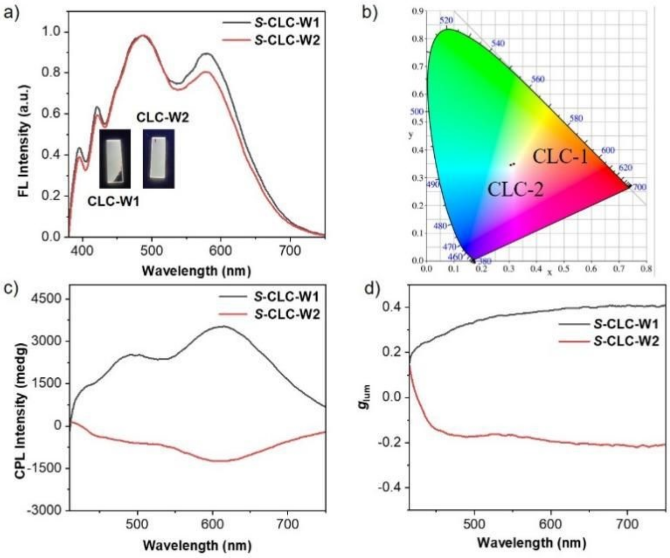

Fig. 5. a) FL intensity of *S*-CLC-W1 and *S*-CLC-W2 (insert: Photograph of the *S*-CLC-W1 and *S*-CLC-W2); b) CIE diagram of the *S*-CLC-W1 and *S*-CLC-W2; c) CPL and d) g_{lum} spectra of *S*-CLC-W1 and *S*-CLC-W2.

Conclusions

CLC-based CPL materials hold profound scientific significance and enormous practical value in chiroptical luminescence and advanced optoelectronic fields, attributed to their facile fabrication and large $|g_{lum}|$ values. To address the inherent single-handedness limitation of natural chirality and expand their application scope in CPL systems, we synthesized a series of full-color dichroic dyes via precise molecular structure engineering. Leveraging this strategy, mirrored full-color CPL and white CPL were readily achieved in natural cholesteric liquid crystals system. This work not only advances the practical application of natural chirality in the CPL field but also provides a novel, sustainable strategy for high-performance CPL devices and flexible optical displays.

Author contributions

View Article Online
DOI: 10.1039/D6SC03246J

C. Li: formal analysis, investigation, methodology, writing – original draft; L. Yang: formal analysis, investigation, methodology; Y. Li: formal analysis, investigation; J. Liu: supervision, investigation; Y. Chen: conceptualization, funding acquisition, supervision, writing review and editing.

Conflicts of interest

There are no conflicts to declare.

Data availability

The data supporting this article have been included as part of the Supplementary Information. Supplementary information: materials and measurements, experimental details, spectral data and additional data. See DOI: [URL–format https://doi.org/DOI]

Acknowledgements

This work was supported by the National Natural Science Foundation of China (22403019), Natural Science Research of the Jiangsu Higher Education Institutions of China (25KJB150012), and research startup fund of Jiangsu Normal University (24XFRS018).

References

1 X. Zhang, Y. Xu, C. Valenzuela, X. Zhang, L. Wang, W. Feng and Q. Li, *Light Sci Appl.,* 2022, **11**, 223.
2 C. Zhang, S. Li, X.-Y. Dong and S.-Q. Zang, *Aggregate.,* 2021, **2**, e48.
3 F. Zinna, G. Pescitelli, and L. D. Bari, *Chirality.,* 2020, **32**, 765-769.
4 L. Yuan, Y. P. Zhang, and Y. X. Zheng, *Sci. China Chem.,* 2024, **67**, 1097-1116.
5 Y. Pan, W. Yin, and Y. Zhang, *Acta Chimica Sinica.,* 2025, **83**, 639-654.
6 F. Furlan, J. M. Moreno-Naranjo, N. Gasparini, S. Feldmann, J. Wade and M.-J. Fuchter, *Nat. Photon.,* 2024, **18**, 658-668.
7 T. Mori, *Chem. Soc. Rev*., 2026, **55**, 1999-2023.
8 G. Zou, Q. Li, Z. Jiang, W. Gao, and Y. Cheng, *Chem. Sci*., 2025, **16**, 11049-11057.
9 C. Zhang, S. Guan, Z.-M. Zhang, W. Gao and Y. Cheng, *Nat. Commun*., 2025, **16**, 6848.
10 Z.-X. Yu, X. W. Chen and M. Li, *Angew. Chem. Int. Ed.,* 2025, **64**, e202517906.
11 Z.-X. Yu, X. W. Chen, C. F. Chen and M. Li, *Angew. Chem. Int. Ed.,* 2025, **64**, e202507802.
12 L. Li, P. Jiang, L. Chen, Y. Li, L. Hu and Y. Cheng, *Chem. Sci.*, 2025, **16**, 21583-21589.
13 J. Li, Y. Liu, Y. Zhang, X. Xin, P. Xing and H. Li, *Nano Lett*., 2025, **26**, 623-631.
14 K.-K. Tan, W. C. Guo, W. L. Zhao, M. Li and C.-F. Chen, *Angew. Chem. Int. Ed.,* 2024, **63**, e202412283.
15 S. Huang, Q. Wu, R. Luo, B. Tan, Y. Yuan and H. Zhang, *Macromolecule*, 2024, **57**, 9017-9029.
16 W. Gong, M. D. Zhou, L. Y. Xiao, C.-Y. Fan, Y.-J. Yuan, Y.-Y. Gong and H.-L. Zhang, *Adv. Opt. Mater.,* 2023, **12**, 2301922.
17 S. Li, Y. Tang, Q. Fan, Z. Li, X. Zhang, J. Wang, J. Guo and Q. Li, *Light Sci. Appl.*, 2024, **13**, 140.
18 Y. Dai, J. Chen, C. Zhao, L. Feng and X. Qu, *Angew. Chem. Int. Ed*., 2022, **61**, e202211822.
19 K. Yao, Z. Wang, P. Wang, Y. Li, L. Hu, Y. Cheng and Z. Geng, *Angew. Chem. Int. Ed*., 2025, **64**, e202420290.
20 Y. Li, J. Luo, X. Zhang, Y. Cheng, Y. Chen and L. Li, *ACS Mater. Lett.*, 2025, **7**, 654-659.
21 F. Wang, O. Gnewou, A. Solemanifar, V.-P. Conticello and E.-H. Egelman, *Chem. Rev.,* 2022, **122**, 14055-14065.
22 F. Gelain, Z. Luo, and S. Zhang, *Chem. Rev.,* 2020, **120**, 13434-13460.
23 Y. Chen, Y. Zhang, H. Li, Y. Li, W. Zheng, Y. Quan and Y. Cheng, *Adv. Mater*., 2022, **34**, 2202309.
24 Y. Li, Y. Chen, H. Li, C. Liu, L. Li, Y. Quan and Y. Cheng, *Angew. Chem. Int. Ed.,* 2023, **62**, e202312159.
25 Y. Li, Y. Chen, J. Luo, Y. Quan and Y. Cheng, *Adv. Mater.*, 2024, **36**, 2312331.
26 C. Guo, J. Zhang, Y. Li, T. Zhang, Y. Liang, J. Wei, X. Ma and X. Han, *ChemistrySelect,* 2026, **11**, e04218.
27 G. Mishra, D. Singh, S. Asthana, H.-S. Tripathi, R. Pandey and M.-D. Pandey, *The Chemical Record*, 2025, **25**, e202500109.
28 M.-T. Sims, L.-C. Abbott, R.-J. Mandle, J.-W. Goodby and J.-N. Moore, *Phys. Chem. Chem. Phys*., 2023, **25**, 10367-10383.
29 M.-T. Sims, R.-J. Mandle, J.-W. Goodby and J.-N. Moore, *Liq. Cryst*., 2017, **44**, 2029-2045.
30 M.-T. Sims, L.-C. Abbott, S.-J. Cowling, J.-W. Goodby and J.-N. Moore, *Phys. Chem. Chem. Phys.*, 2017, **19**, 813-827.
31 M.-T. Sims, L.-C. Abbott, S.-J. Cowling, J.-W. Goodby and J.-N. Moore, *J. Phys. Chem. C.*, 2016, **120**, 11151-11162.
32 J. Ren, L. Ji, C. Jiang, P. Duan, G. Ouyang and M. Liu, *CCS Chem*., 2025, **7**, 3664-3675.
33 Z.-W. Luo, H. Ji, X. Jin, J. Song, J.Z.-Q. Yu, P. Duan and T. Zhao, *Nat. Commun.,* 2025, **16**, 9960.
34 M.-J. Ji, W.-L. Zhao, M. Li and C.-F. Chen, *Nat. Commun.*, 2025,**16**, 2940.
35 K. Akagi, *Chem. Rev.* 2009, **109**, 5354-5401.
36 Y. Chen, Y. Li, H. Li, L. Li, Y. Quan and Y. Cheng, *Sci. China Chem.*, 2024, **67**, 1250-1255.
37 Y. Li, Y. Chen, J. Luo, Q. Li, Y. Quan and Y. Cheng, *Chin. Chem. Lett.*, 2024, **35**, 109864.
38 Y. Chen, L. Li, K. Yao, C. Fu, Y. Li and Y. Cheng, *Adv. Opt. Mater.*, 2025, **13**, 2403100.
39 G. Albano, G. Pescitelli, and L. D. Bari, *Chem. Rev.* 2020, **120**, 10145-10243.
40 P. Zhao, H.-Y. Lu, and C.-F. Chen, *Chem. Soc. Rev.,* 2025, **54**, 8534-8554.
41 C.-H. Guo, L. Feng, C.-F. Chen and M. Li, *Angew. Chem. Int. Ed.,* 2025, **64**, e202516018.
42 R. Ren, Y. Pan, H.-X. Wang and M. Liu, *Chin. Chem. Lett.*, 2025, **37**, 111060.
43 P. Zhao, W.-C. Guo, H.-Y. Lu and C.-F. Chen, *Angew. Chem. Int. Ed*., 2025, **64**, e202424918.
44 X. Wang, Q. Song, Z. He, G. Zhang, T. Miao, X. Cheng and W. Zhang, *Chin. Chem. Lett*., 2025, **36**, 110047.
45 X. Meng, S. Lin, and J. Guo, *Acc. Chem. Res.*, 2025, **58**, 2586-2599.
46 Y. Zhang, G.-K. Tian, D. Li, Z.-H. Jiang, Y. Quan and Y. Cheng, *Laser Photonics Rev*., 2024, **18**, 2400223.
47 H.-R. Fu, R.-Y. Zhang, C.-Y. Wei, S. Liu, J.-Y. Xu, X. Zhu, J. Wei, Q.-R. Ding and L.-F. Ma, *Chem. Commun.,* 2024*,* **60**, 10212-10215.
48 Y. Zhang, Y. Li, Y. Quan, S. Ye and Y. Cheng, *Angew. Chem. Int. Ed.*, 2023, **62**, e202214424.
49 X. Gao, J. Wang, K. Yang, B. Zhao and J. Deng, *Chem. Mater.*, 2022, **34**, 6116-6128.

View Article Online
DOI: 10.1039/D6SC03246J

The data supporting this article have been included as part of the Supplementary Information.